Developmental Biology 451 (2019) 40–52

Contents lists available at ScienceDirect

Developmental Biology

journal homepage: www.elsevier.com/locate/developmentalbiology

Review article

Multi-scale regulation of cell branching: Modeling morphogenesis

Jing Li[a], Taeyoon Kim[a], Daniel B. Szymanski[b,c,d,*]

[a] Weldon School of Biomedical Engineering, Purdue University, West Lafayette, IN 47907, United States
[b] Department of Botany and Plant Pathology, Purdue University, West Lafayette, IN 47907, United States
[c] Department of Biological Sciences, Purdue University, West Lafayette, IN 47907, United States
[d] Department of Agronomy, Purdue University, West Lafayette, IN 47907, United States

ARTICLE INFO

Keywords:
Polarized growth
Microtubule
Cytoskeleton
Cell wall biomechanics
ARP2/3
Computational modeling

ABSTRACT

Plant growth and development are driven by extended phases of irreversible cell expansion generating cells that increase in volume from 10- to 100-fold. Some specialized cell types define cortical sites that reinitiate polarized growth and generate branched cell morphology. This structural specialization of individual cells has a major importance for plant adaptation to diverse environments and practical importance in agricultural contexts. The patterns of cell shape are defined by highly integrated cytoskeletal and cell wall systems. Microtubules and actin filaments locally define the material properties of a tough outer cell wall to generate complex shapes. Forward genetics, powerful live cell imaging experiments, and computational modeling have provided insights into understanding of mechanisms of cell shape control. In particular, finite element modeling of the cell wall provides a new way to discover which cell wall heterogeneities generate complex cell shapes, and how cell shape and cell wall stress can feedback on the cytoskeleton to maintain growth patterns. This review focuses on cytoskeleton-dependent cell wall patterning during cell branching, and how combinations of multi-scale imaging experiments and computational modeling are being used to unravel systems-level control of morphogenesis.

1. . Introduction

Plants are sessile organisms that convert solar radiation to chemical energy that fuels growth and development. Cell production in meristems and extended phases of irreversible polarized cell expansion drives morphogenesis as the plant continuously explores and responds to its environment. Plants are intricate biomechanical machines; from relatively simple low profile mosses that colonize moist habitats to the tallest angiosperms that out-compete neighbors by intercepting photosynthetically active solar radiation. Cells with specialized shapes and customized mechanical properties are the fundamental building blocks for plant development. Plant and cell architectures have also been strongly modified by human selection. For example, the angle and morphology of maize leaves enable high planting densities that have driven most of the increases in yield per acre. At the spatial scale of single cells, human selection has generated cotton cultivars in which individual cells have centimeter length-scales, low diameter, and high tensile strength. Optimized plant architectures continue to be a plant breeding and genetic engineering target as the list of crops that can have the potential to disrupt the pharmaceuticals, bioenergy, and chemical engineering industries continues to expand. Therefore, understanding the orchestration of multi-scale dynamics behind cell growth and tissue patterning is of great importance and benefit.

Morphogenesis in plants is unique, and driven by the biomechanical properties of cells, tissues, and organs. As sessile organisms, their form arises from a fixed location where the seed germinates, and the root and shoot develop in opposite directions. Plants grow rapidly and move through space, but the movement and development are not driven by the migration of individual cells or groups of cells relative to one another. Instead, meristems generate groups of progenitor cells that are progressively displaced from the meristematic zone as they divide and grow. Growth is symplastic since they expand as groups of cells that are mechanically coupled to their neighbors through a pectin- rich middle lamella. After plant cells exit the cell cycle, many of them undergo multiple rounds of endoreduplication (Melaragno et al., 1993; Szymanski and Marks, 1998), and 10–100-fold increases in cell volume strongly influence the size and shape of the organ (Foard and Haber, 1961). For example, in elongating roots and stems, the coordinated anisotropic expansion of files of cells drives organ elongation. The overall shape and local boundaries of most cell types are relatively simple and rather smooth, lacking filopodia-like projections that are present in animal cells. Most plant cell types associated with organ elongation are cylindrical, and

* Corresponding author at: Department of Botany and Plant Pathology, Purdue University, West Lafayette, IN 47907, United States.
E-mail address: szymandb@purdue.edu (D.B. Szymanski).

https://doi.org/10.1016/j.ydbio.2018.12.004
Received 15 October 2018; Received in revised form 29 November 2018; Accepted 3 December 2018
Available online 05 December 2018
0012-1606/

ground tissues are comprised primarily of simple polyhedral cells. As the plant develops, a subset of cell types synthesize highly thickened and/or lignified secondary cell walls after cell expansion ceases to generate mechanical stability to the stems and leaves (Esau, 1977).

Many plant cell types, from the most basal algal species to flowering plants, have elaborate branched morphologies that enable specialized mechanical, transport, or signaling functions (Dolan et al., 1993; Leliaert et al., 2012; Sahoo and Baweja, 2015; Szymanski, 2014; Zhou et al., 2017). Selected examples include the branching of unicellular leaf trichomes that act as physical deterrents to insect feeding (Fig. 1a, b). The branched and highly lignified sclereid cells provide mechanical stability to a tissue (Fig. 1c). Individual cells branch in filamentous algae and moss (Fig. 1d) to generate complex 3D morphologies to efficiently colonize a substrate. Specialized cells in the root epidermis branch at specific locations to generate root hairs that greatly increase the absorptive capacity of the organ (Fig. 1e). In the context of a tissue, leaf epidermal cells in many dicot species generate a branched, interdigitated morphology to promote polarized growth and mechanical stability of thin durable leaves (Fig. 1f). Genetic screens in model plant species are generating an ever-growing parts list of proteins and cell wall polymers that pattern growth. It is becoming possible to discover the basic design principles for plant cell shape control and generate engineering strategies to specify cells and even tissues with desired shapes. This review will introduce basic concepts of plant cell shape control and then focus on illustrative examples in which the combined use of mutants, live cell imaging, and computational simulations of the plant cell wall mechanics is driving the cell morphogenesis field forward.

2. Basic mechanics of cell expansion: cell walls and cytoskeletal patterning

The patterns of cell growth are the output of complex interactions between the hydraulic properties of the cell and the local rheology and cytoplasmic patterning of the cell wall. Most plant cells use a diffuse growth mechanism in which secretion, cell wall synthesis, and cell expansion occur broadly over the cell surface (Cosgrove, 2018). Cell expansion is driven mainly by water transport and turgor pressure (Cosgrove, 1993; Ray et al., 1972). Osmotically active solutes in the cytoplasm drive water transport into the cell through aquaporins localized on a plasma membrane, resulting in isotropic cytoplasmic turgor pressure. The stiffness of the cell wall limits cell expansion, leading to cell wall stress. With turgor pressures in the range of 0.5–1 MPa, the magnitude of wall stress is estimated to be ~10 MPa (Cosgrove, 1993; Forouzesh et al., 2013; Yanagisawa et al., 2015). The magnitudes and directions of stresses on the cell wall are not uniform and vary depending on several factors, such as cell geometry and the thickness and material properties of a cell wall (Jordan and Dumais, 2010; Yanagisawa et al., 2015). Cell wall material properties are affected by pH, free radicals, and enzymes that can alter its extensibility (Cosgrove, 2005). During growth, cell wall assembly is coupled with cell expansion so that cell wall thickness is maintained during expansion. Cellulose microfibrils within the wall play a major role in defining its material properties (Baskin, 2005). Within elongating cells, bundles of long cellulose microfibrils are often aligned in the cell wall in transverse directions roughly perpendicular to the long axis of the cell. This results in highly anisotropic material properties of cell wall, making the it much stiffer in the transverse directions. Cellulose fibers are embedded in a polysaccharide wall matrix. Pectin is one matrix component that interacts with cellulose (Wang et al., 2015), and the highly regulated material properties of pectin have a strong influence on cell morphogenesis (Hocq et al., 2017). Generation of a new cell growth axis during branching requires local modification of the cell wall so that a subregion selectively yields to turgor pressure.

The local material properties of the cell wall are patterned by the microtubule and actin cytoskeletons (Szymanski and Cosgrove, 2009). The orientations of cellulose microfibrils are influenced by cortical

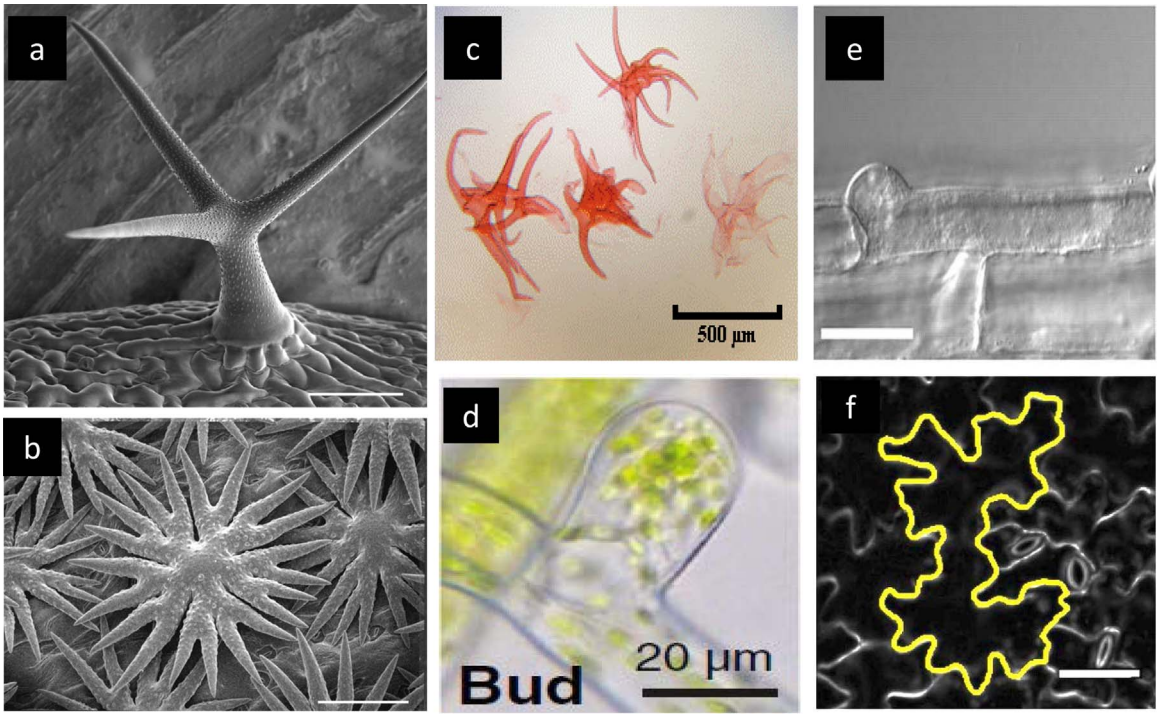

Fig. 1. Branched cell morphologies in various plant cell types. (a-b) Scanning electron micrographs of leaf trichomes in (a) Arabidopsis and (b) *Physaria goodrichii*. Scale bars = 100 µm [reprinted with permission from (Beilstein and Szymanski, 2004)]. (c) Star-shaped sclereids isolated from *N. lutea* stems [reprinted with permission from (Marrotte et al., 2012) Copyright © 2011 Elsevier B.V. Published by Elsevier B.V. All rights reserved]. (d) Formation of a branch initiation site during filamentous growth in the moss *Physocmitrella patens* [reprinted with permission from (Russell et al., 2017)]. (e) Cell branching and bulge formation during root hair initiation in Arabidopsis. Root hair initials form at the distal ends of cylindrically shaped epidermal cells. Scale bar = 40 µm [reprinted with permission from (Ringli et al., 2002) Copyright © 2002 American Society of Plant Biologists. All rights reserved]. (f) Highly lobed leaf epidermal pavement cells in Arabidopsis (Wu et al., 2016) [reprinted with permission from (Belteton et al., 2018)]. The epidermal tissue is comprised of highly interdigitated pavement cells that morph from a simple polyhedron into a jig-saw-puzzle piece shape with variable numbers of lobes. Scale bar = 50 µm.

microtubules which are tightly associated with the plasma membrane forming essentially a two-dimensional array on a face of the cell cortex (Shaw et al., 2003b; Wasteneys and Ambrose, 2009). A correlation between the alignments of microtubules and cellulose microfibrils was observed for the first time in the electron microscope (Hepler and Newcomb, 1964; Ledbetter and Porter, 1963). Microtubules influence the patterns of cellulose synthesis by positioning the insertion of cellulose synthase complexes adjacent to microtubules and by guiding the trajectory of active complexes as they move in the plane of the plasma membrane. Fully assembled cellulose synthase complexes (CESA) are delivered to the plasma membrane via specialized vesicles. Cellulose microfibrils are synthesized by an oligomeric CESA localized in the plasma membrane (Gutierrez et al., 2009; Paredez et al., 2006; Purushotham et al., 2016). Two-color live cell imaging has shown that microtubules are coupled to CESA, and the organization of microtubules influences the trajectories of movement of CESA particles (Gutierrez et al., 2009; Li et al., 2012; Paredez et al., 2006). The co-alignment of microtubule and cellulose microfibril is a golden rule for the complicated machinery that induces cell branching and morphogenesis across wide spatial scales.

Besides the patterning mechanism based on microtubules, plant cells use polarized vesicle trafficking and the actin cytoskeleton to generate subcellular gradients in the material properties of cell wall that locally modulate the rate and/or direction of cell wall expansion during growth (Bascom et al., 2018; Yanagisawa et al., 2015). Specialized cell types, such as root hairs, pollen tubes, and protonema in the mosses, use a tip-growth mechanism to modulate cell wall mechanics at the extreme apex. An actin-based pattern of polarized transport generates an apical zone where new cell wall matrix and pectin-modifying enzymes are locally secreted to decrease the modulus and increase the extensibility of the cell wall (Bascom et al., 2018; Fayant et al., 2010; Hepler et al., 2013). In the moss *Physcomitrella patens*, an actomyosin-dependent vesicle cluster is dynamically positioned at the cell apex to direct secretion to a small patch at the cell apex (Bibeau et al., 2017; Wu and Bezanilla, 2018). In root hairs and pollen tubes, cell wall extensibility appears to be controlled in part by spatially varying the chemical properties of pectin at the apex (Bosch et al., 2005; Levesque-Tremblay et al., 2015; Rounds et al., 2011). The precise function of actin filaments in cells that use a diffuse growth mechanism has been difficult to nail down. The actin network influences the general patterns of long-distance intracellular transport and pectin secretion (Leucci et al., 2007), and a subset of specialized cortical actin filaments have the potential to organize actin bundles at a cellular scale to ensure that transport to the cortex is broadly distributed throughout the cell cortex (Yanagisawa et al., 2015).

3. Leaf hair morphogenesis: cellular control of branch initiation

Leaf trichomes are morphologically diverse structures that are often branched. They emerge from protodermal cells in the leaf epidermis and differentiate into cell types that can accumulate specialized metabolites that deter insect feeding (Levin, 1973). Stellate unicellular trichomes, like those of Arabidopsis, serve as a physical defense against insect attack (Mauricio, 1998; Sato et al., 2014), influence the reflective properties and gas exchange of the leaf, affect photosynthesis (Schreuder et al., 2001; Suo et al., 2013), and can sense mechanical forces on the leaf surface (Zhou et al., 2017).

The leaf hair cell fate is controlled by an evolutionarily conserved triad of transcription factors and negative regulators that determine the number and spacing of trichoblasts (Szymanski et al., 2000). The cell biology of cell trichome shape control is best developed in Arabidopsis, in which trichoblasts undergo additional rounds of endoreduplication and are converted into an enlarged spherical cell that generates a polar growth axis which morphs into a cylindrical peg perpendicular to the leaf axis (Hulskamp et al., 1994). Branch initiation requires an intact microtubule cytoskeleton and numerous genes involved in vesicle trafficking (Falbel et al., 2003) but surprisingly occurs independently of the actin cytoskeleton (Mathur et al., 1999; Szymanski et al., 1999). Mutations and inhibitors that stabilize the microtubule cytoskeleton increase trichome branch number (Mathur and Chua, 2000; Mathur et al., 1999; Sambade et al., 2014). Many papers refer to the branch point number as if the growing cell bifurcates during branching, but in fact the elongating stalk is partially consumed as a new growth axis is generated along the flank of the expanding cell (Szymanski et al., 1998, 1999). Branch initiation occurs sequentially on the elongating stalk to yield a regular spacing of ~120°. Leaf trichome branch number and shape can vary greatly among related species (Fig. 1a, b).

The means by which microtubules control branch initiation is not entirely clear. Expectedly, cellulose microfibrils are required, considering a point mutation in a CESA subunit reduces cellulose crystallinity and eliminates branching (Fujita et al., 2013). Elongating trichome stalks and emerging trichome branches have a microtubule-depleted zone (MDZ) at the extreme apex and a collar of transverse cortical microtubules that is positioned near the branch apex (Beilstein and Szymanski, 2004). The position or density of the collar appears to be significant because the *ANGUSTIFOLIA* (*AN*) mutant has a longitudinally expanded transverse microtubule collar and has an obvious branch number defect (Folkers et al., 2002). A detailed live cell imaging analysis of microtubules during branch formation showed that the incipient branch bulge forms at the proximal flank of the microtubule collar (Sambade et al., 2014). The trichome stalk and branches elongate via a highly polarized diffuse growth mechanism (Schwab et al., 2003; Szymanski et al., 1999; Yanagisawa et al., 2015). The distal boundary of the transverse microtubule collar would be expected to pattern a domain of the cell wall with a sharp gradient in the degree to which cellulose microfibrils are aligned. Within the collar, newly synthesized cellulose microfibrils would be highly aligned, whereas outside of the collar, the newly synthesized fibers would be expected to be randomly oriented. A validated finite element (FE) mechanical model of a similarly patterned trichome branch cell wall predicts that this transition zone generates a robust narrow band of elevated cell wall stress (Yanagisawa et al., 2015). Perhaps, a combination of cell size (which also affects cell wall stress) and cellulose fiber alignment gradients are sensed by cytoplasmic factors that can activate proteins which locally loosen the existing cell wall or position the endomembrane system to secrete new cell wall components that assemble into a more extendible wall. Cortical microtubule-dependent exclusion of factors that promote branch initiation is another possible control mechanism. The DOCK-family ROP/Rac guanine nucleotide exchange factor SPIKE1 (SPK1) is a tip-localized signaling protein that is excluded from microtubule-rich cortical domains (Yanagisawa et al., 2018). SPK1 promotes branch initiation independent of its ability to activate ARP2/3-dependent actin polymerization (Basu et al., 2008). Similar interactions among cell geometry, cell wall stress, and cytoskeletal patterning may control the spacing of subsequent branching events on the same cell.

Trichome morphology mutants have been a treasure trove for gene discovery and genetic analyses of branching (Fig. 2). The transcription factors GL1-TTG- and GL3 reside at the top of a regulatory hierarchy that controls both cell fate (the patterning of trichome initiation) and promotes endoreduplication in developing trichoblasts. The DNA content of trichome cells ranges from 16 C to 64 C, and endoreduplication is strongly correlated with branch number (Schnittger et al., 1998; Szymanski and Marks, 1998). The STICHEL (STI) is a plant specific protein that appears to link endoreduplication and DNA content to cell morphology (Ilgenfritz et al., 2003). STI is a tip-localized protein that may function in a heteromeric complex which includes another tip-localized protein BRANCHLESS TRICHOME (BLT) (Marks et al., 2009). BLT and STI genetically and physically interact (Kasili et al., 2011; Xi et al., 2018), and over-expression of either is sufficient to increase trichome branch number without a detectable increase in endoreduplication (Kasili et al., 2011; Marks et al., 2009). Therefore, a STI-BLT

complex may be an important growth control rheostat that explains morphological diversity in related species (Mazie and Baum, 2016). The Chromatin Assembly Factor-1 (CAF-1) gene may function upstream of the BLT-STI complex, as the increased branch number of CAF-1 mutants is suppressed in a double mutant combination with *sti* (Exner et al., 2008). The mechanism by which STI activity and endoreduplication are linked to the microtubule cytoskeleton and cell branching is not known. However, given that *BLT* and *STI* are epistatic to most known increased branching mutants (but not *NOK*) that increase trichome branching (Ilgenfritz et al., 2003; Exner et al., 2008; Kasili et al., 2011), and that STI overexpression can increase trichome branch number (Ilgenfritz et el., 2003), this predicted protein complex has important signaling and patterning functions during branch formation.

Many mutations in tubulin genes and microtubule-associated proteins have trichome branch number phenotypes (Buschmann and Lloyd, 2008). Two known microtubule-associated proteins, the microtubule severing protein katanin (FRAGILE FIBER 2/FRA2 (Burk et al., 2001)) and the minus-end-directed kinesin motor protein ZWI/KCBP (Oppenheimer et al., 1997; Reddy et al., 1996), have reduced trichome branch number phenotypes. ZWI/KCBP has a small C-terminal domain that is a binding site for the EF-hand domain-containing Ca2+ sensor proteins KIC (Reddy et al., 2004) and CML42 (Dobney et al., 2009). Genetic data are consistent with a model in which KIC and CML42 negatively regulate ZWI/KCBP in a calcium-dependent manner. Surprisingly, deletion of this C-terminal domain of ZWI/KCBP has a minor effect on its function, causing only a small increase in the proportion of trichomes having four branches (Tian et al., 2015). A putative microtubule catastrophe-inducing *KINESIN13A* mutant has an increased trichome branch number (Lu et al., 2005). It has been shown in other cell types and in transient expression experiments that KINESIN13A is regulated by a ROPGEF-ROP/RAC signaling module that locally recruits and activates KINESIN13A (Oda and Fukuda, 2012, 2013a, 2013b). A similar signaling module employing either SPK1 or a PRONE-domain GEF may locally activate KINESIN13A in trichomes (Fig. 2). ROP signals may also control the microtubule-severing activity of FRA2 (Lin et al., 2013). Clearly, there is much to be learned about how a feedback between layers of small GTPase and Ca^{2+} signaling and the cell wall determines the location and number of branch initiation sites.

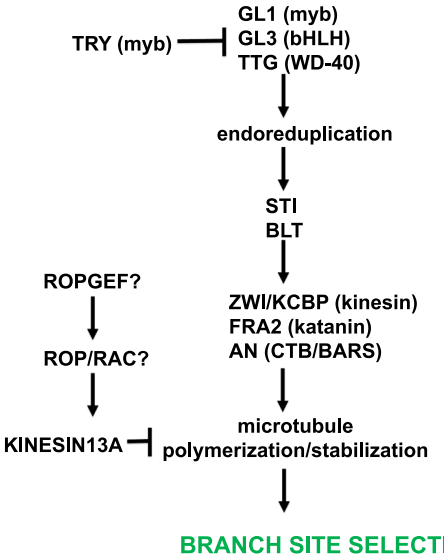

Fig. 2. Genetic model of branch initiation that includes genes that link endoreduplication with microtubule-based branch initiation. Cell size and the number of branches are positively correlated with the DNA content of cell. The transcription factor complex of GL1-GL3-TTG promotes endoreduplication, and TRY inhibits the complex. The STI and BLT proteins are required to couple endoreduplicatoin and branch initiation. They may function as upstream of the known microtubule binding proteins ZWI/KCBP and FRA2. The AN gene is required to organize an apically concentrated microtubule array. Localized microtubule stabilization promotes branch initiation at an adjacent location. KINESIN13A promotes microtubule catastrophe and antagonizes microtubule-dependent branch initiation. Arrows indicate positive regulatory interactions, and blocked lines indicate negative regulation. Text in green indicates the growth output of the pathway.

4. Branch morphogenesis: cellular control and a mechanical model

Many branch initiation genes also affect branch morphogenesis (Fig. 3). After the branch bulge forms, the apical MDZ is maintained, and a new collar of transverse microtubules forms at the base of the bulge and the branch elongates (Sambade et al., 2014; Yanagisawa et al., 2015) (Fig. 4a). This microtubule array promotes an extended (~14 h) phase of highly anisotropic diffuse growth that converts the bulge to a prolate ellipse and eventually generates a miniaturized version of the mature trichome cell (Yanagisawa et al., 2015).

Detailed live cell imaging analysis of the geometry of the branch shape change, subcellular patterns of cell growth, and cell wall thickness gradients were used to parameterize and validate an FE model of the developing branch (Fig. 4b) (Yanagisawa et al., 2015). Physical measurements of turgor pressure and cell wall relaxation times in the leaf epidermis were also used to develop the model (Forouzesh et al., 2013; Hayot et al., 2012). In this FE model, the cell wall was modeled as axisymmetric linear viscoelastic shell with an initial geometry of a prolate ellipse. The material model contained a

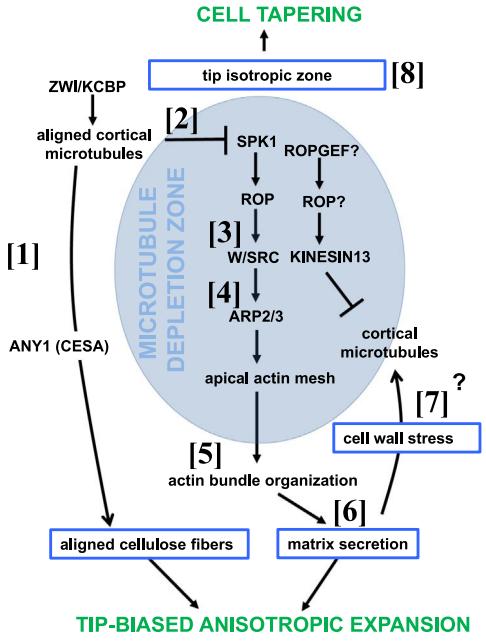

Fig. 3. A combined genetic and biomechanical model for branch morphogenesis. Key activities are numbered and defined below. Transverse cortical microtubules pattern cellulose microfibrils in the cell wall that generate highly anisotropic cell expansion along the branch flanks (1). Cortical microtubules near the branch apex also confine SPK1 signaling within the MDZ (2). In a fully activated state, SPK1 recruits and activates the W/SRC (3) and ARP2/3 complexes (4) to generate a cortical actin meshwork that has been shown to orient bidirectional actin bundles (5) that determine the cytoplasmic patterns of flow and secretion (Yanagisawa et al., 2015). The organized cellular flow pattern enables balanced synthesis of aligned cellulose fibers and cell wall matrix secretion during tip-biased diffuse growth. The microtubule depletion zone of the branch apex (labeled as a light blue circle) is predicted to have isotropic cellulose fibers. The radius of curvature of the cell wall and the size of microtubule depletion zone are tightly coupled. This coupling is sensitive to a slow actin dependent process that occurs at times scales > 5 h. The slow process may be cell wall secretion that enables accurate feedback control from the cell wall to the microtubule cytoskeleton. Localized cell wall stress gradients at the boundaries of the microtubule depletion zone (7) may enable the cell to integrate cell wall geometry with microtubule depolymerization for accurate branch tapering (8). Arrows indicate positive regulatory interactions, and blocked lines indicate negative regulation. Text in blue boxes indicates the types of cell wall modification that underlies different growth outputs which are defined with green text.

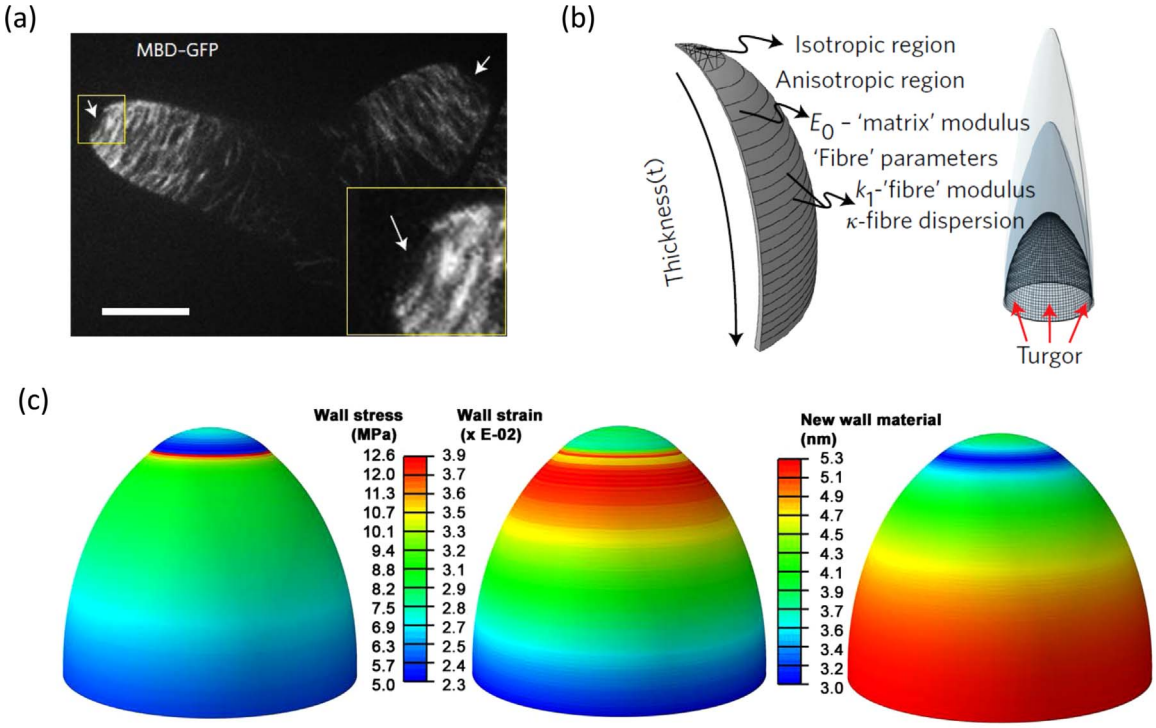

Fig. 4. A validated finite element model of branch morphogenesis. (a) A confocal image of the microtubule network in a young trichome branch. Arrows mark a clear microtubule depleted zone at the trichome branch tip and a transverse array of microtubules along the apical flanks. (b) A schematic of the finite element shell model of trichome cell wall. On the left panel, the key parameters that influence branch morphogenesis are listed; a cell wall thickness gradient, aligned fibers in the branch flank, and an apical isotropic region representing the microtubule depleted zone collectively generate a branch that tapers using a tip-biased anisotropic diffuse growth mechanism. The right panel illustrates the different shapes of the simulated trichome branch at subsequent modeling cycles. (c) Heat maps for the wall stress (left), maximal principal strain (middle), and the new material budget to restore cell wall thickness after a single growth simulation cycle (right). The shallow bias toward increased material at the base is driven by its higher radius and thickness compared to other regions of the cell. Figures adapted from (Yanagisawa et al., 2015).

matrix coupled with a network of anisotropic hyperelastic fibers. The modulus coupling of the matrix and fiber network in the model was estimated based on experimentally measured changes in cell geometry and fiber angle distributions estimated from microtubule angles (see Fig. 2d in:Yanagisawa et al., 2015).

Branch growth was simulated as a sequence of iterated FE cycles in which the shell was loaded with an internal force equal to turgor pressure of epidermal cells, the wall relaxed to an equilibrium state, the resultant wall geometry was re-meshed with a new FE grid, and the wall properties at the corresponding locations in the new shell were reset to the original values (Fig. 4b, right). The shape and local strain behaviors of the simulated and experimentally measured cell are compared to identify physical parameters that have power in terms of controlling the rates and patterns of shape changes. These predicted parameters are then experimentally tested, and the model is refined. For example, the trichome branch model predicted a specific threshold for transverse fiber alignment that was required to generate the observed pattern of highly anisotropic branch elongation. The experimentally measured distribution of cortical microtubule angles exactly matched this prediction (Yanagisawa et al., 2015). The validated model generates useful predictions about the patterns of cell wall tensile stress, spatial patterns of strain/growth, and spatial material delivery budgets that are needed to support branch morphogenesis (Fig. 4c).

The apical MDZ in the developing branch has an importance for both cell signaling and the mechanics of cell shape changes. The MDZ persists throughout branch morphogenesis (Fig. 4a), and its geometry is strongly correlated with the branch tip radius of curvature that becomes progressively smaller as the cell tapers (Yanagisawa et al., 2015). This correlation likely reflects both cytoplasmic patterning of the cell wall and a mechanical feedback from the wall to the protein machineries that define the size of the MDZ. The MDZ generates an apical cell wall patch with isotropic fibers, and the progressive constriction of this zone is sufficient to explain the tapering process during which the branch bulge is refined to a sharp tip that is presumably more effective as an insect feeding deterrent. The factors that control the size and axial centering of the MDZ are not known. Spatial gradients of cell wall stress that were discussed in the context of branch initiation may also contain information that is decoded by the proteins defining the geometry of the MDZ. Since the MDZ is present in SPK1 null mutants (Yanagisawa et al., 2018), it is possible that PRONE-domain GEFs and ROP signaling through KINESIN13 link the behaviors of the MDZ with the geometry of the cell wall.

The MDZ is also a location at which the actin filament-nucleating ARP2/3 complex is clustered and activated (Yanagisawa et al., 2015). In angiosperms, and perhaps in all plant species, ARP2/3 is activated solely by the WAVE/SCAR complex (Yanagisawa et al., 2013). In Arabidopsis epidermal cells, the WAVE/SCAR complexes associate with organelle surfaces (Kotchoni et al., 2009; Zhang et al., 2013a, 2013b). In a fully activated state, ARP2/3 generates an apical actin meshwork. Through unknown mechanisms, the apical meshwork organizes a population of cytoplasmic actin bundles to organize bidirectional flow and a broad cortical distribution of the endomembrane system at the spatial scale of the cell (Yanagisawa et al., 2015). This actin organization is not supporting tip growth. It is directing a broadly dispersed material delivery budget that was calculated from the FE model based on cell geometry, cell wall thickness, and subcellular growth patterns (Fig. 4c). The model predicted the existence of a base to tip cell wall thickness gradient to explain the observed apical bias in the rates of diffuse growth, and this was validated using electron microscopy and direct measurements of wall thickness along the branch length (Yanagisawa et al., 2015). In ARP2/3 mutants cell wall, gradients are not present and the patterns of subcellular cell wall strain are severely altered. ARP2/3 organizes a cellular scale acto-myosin transport and cell wall matrix delivery system to allow the cell to

integrate and coordinate cell shape, growth rates, and cell wall material properties. Interestingly, mutation of ARP2/3 and removal of the apical actin cap do not eliminate the MDZ. The size and position of the MDZ become more random both in ARP2/3 mutants (Yanagisawa et al., 2015) and only after extended (~5 h) treatments with the actin-depolymerizing drug latrunculin B (Yanagisawa et al., 2018). These results suggest that ARP2/3 and actin affect the MDZ indirectly, perhaps by altering spatial patterns of cell wall matrix delivery and the ratio of matrix to fiber modulus in the cell wall (Leucci et al., 2007), which is predicted to be important for cell shape control (Yanagisawa et al., 2015).

An important feedback control mechanism between the microtubule and actin cytoskeletons was recently discovered (Fig. 3, step 2). SPK1 was shown to have GEF activity in the branch apex and to recruit and activate the WAVE/SCAR complex (Yanagisawa et al., 2018). SPK1 and WAVE/SCAR are clustered at short lived (life times of ~mins or occasionally tens of minutes) cortical nodules that are anchored to the plasma membrane. The nodules may correspond to ER-plasma membrane contact sites based on previous immunolocalization results (Zhang et al., 2010) and the persistence of ER markers in the apex of developing branches. SPK1 signaling nodules are always found within the MDZ. However, when microtubules were depolymerized, the cortical domain that was competent to cluster SPK1 slowly spreads down the cell flank (Yanagisawa et al., 2015). These results indicate that the apical boundary of the cortical microtubule collar serves as a spatial landmark to dynamically define the boundary limits for SPK1-dependent ARP2/3 activation. This mode of control provides a mechanism to achieve cellular-scale control of the microtubule and actin cytoskeletal systems.

5. Branch formation in tip-growth systems: root hairs and moss caulonema

Plant cells are also capable of generating branched structures that are converted to tip-growing structures. Root hair initiation is a classic example. The developing root has a clear developmental gradient along the length of the root (Dolan et al., 1993). Files of adherent epidermal cells are displaced away from the root tip by a combination of cell division and cell expansion. As cell expansion ceases at a predictable distance from the root meristem, root hairs emerge as a broad bulge at the rootward end of highly elongated cylindrically shaped epidermal cell that is converted to a tip-growing cell which propagates a self-similar shape during an extended phase of cell elongation. Root hairs have important nutrient and ion uptake functions for the plant (Fig. 1e). The cell and developmental biology of root hair have been the subject of detailed reviews (Grierson et al., 2014; Honkanen and Dolan, 2016). We will focus on the initial bulge formation event that generates a branched cell.

The mechanical properties of the root-hair forming cell wall and the hair initiation site are highly specialized. Numerous mutations that affect cellulose synthesis cause ectopic cell bulging and defects in root hair initiation (Arioli et al., 1998; Burn et al., 2002; Howles et al., 2006). CESA6/PROCUSTE1 is expressed in all cell files, but the cell bulging and root hair initiation defects are expressed selectively in hair-forming files, suggesting that the material properties of the hair cell files are unique (Singh et al., 2008). Several ions and enzyme activities have been implicated in specifying the location for hair initiation. The ROOTHAIR DEFECTIVE2 (RHD2) mutant affects the number, location, and length of root hairs (Grierson et al., 1997). RHD2 encodes an NADPH oxidase that concentrates at pre-initiation sites (Foreman et al., 2003) and functions in concert with apoplastic PEROXIDASEs (Mangano et al., 2017) to promote localized cell expansion. Generation of localized reactive oxygen is an evolutionarily conserved strategy for root hair initiation and outgrowth (Carol and Dolan, 2006; Nestler et al., 2014; Wang et al., 2018). Reactive oxygen signaling corresponds to a convergence point of plant hormones ethylene and auxin (Feng et al., 2017; Mangano et al., 2017), both of which have long been known to affect root hair initiation (Massucci and Schiefelbein, 1994). Expansins are another class of well-known wall loosening enzymes. Expansins are preferentially expressed in hair cell files (Cho and Cosgrove, 2002), and the protein accumulates at root hair initiation sites (Baluska et al., 2000). The cell wall domain that is converted to the root hair bulge is also acidified by the local activation of H^+-ATPases (Bibikova et al., 1998). Low pH activates expansins and further implicates this wall loosening enzyme (Cosgrove, 2000); however, genetic data supporting this function is currently lacking.

The bulge site also displays dramatic localized changes in the organization of the cytoplasm. The cortical microtubule array is locally disrupted at the site of bulge formation (Baluska et al., 2000; Pietra et al., 2013). The microtubule-associated proteins SABRE and CLASP influence the location of the bulge site (Pietra et al., 2013). The endomembrane system is rearranged at the bulge site. The phosphoinositide PI(4,5)P2 becomes concentrated in the plasma membrane at the bulge site (Kusano et al., 2008), and the ER appears to become clustered and stabilized (Ridge et al., 1999). ROP small GTPase signaling is certainly involved in bulge site selection. Several labs have shown that ROP accumulates at pre-bulge sites (Jones et al., 2002a; Molendijk et al., 2001; Pietra et al., 2013), and mutation of a guanine nucleotide dissociation inhibitor leads to the formation of ectopic bulge initiation sites on individual cells (Carol et al., 2005). Therefore, functional ROP signaling is required to select and maintain a single stable branch initiation site. Unlike the leaf trichome system, the actin cytoskeleton plays a prominent role in bulge initiation. Several actin binding proteins have been shown to concentrate at bulge initiation sites (Baluska et al., 2000; Kiefer et al., 2015), and actin mutants have major effects on the positioning, stability, and functionality of bulge initiation sites (Kiefer et al., 2015; Ringli et al., 2002). The particular actin meshwork that is associated with bulge formation is not known as live cell probes for actin failed to detect a clear filament meshwork or actin bundle system associated with the bulge (Kiefer et al., 2015). This is similar to the case in young leaf trichome branches in which the apical actin meshwork is clear in fixed, detergent extracted cells, but almost impossible to resolve using the ABD2 and Lifeact live cell probes (Yanagisawa et al., 2015). Direct translational fusions of GFP to actin may provide a way to image actin meshworks that cannot be detected by probes that bind to the sides of actin filaments (Kijima et al., 2018).

The organization of the actin cytoskeleton during cell branching has been beautifully resolved during filamentous growth in the moss *Physcomitrella patens*. During the filamentous stage of their life cycle, tip growing chloronema and caulonema cells elongate and divide, generating linear arrays of cells that efficiently colonize the environment. The most apical cell does not branch, but after cell division, the more proximal daughter cell can generate a new growth axis near the recently formed cell division site (Fig. 1c). The branch is initiated as a defined bulge in the cell wall expands further. Cell division occurs subsequently near the site of bulge initiation (Cove and Knight, 1993; Wu et al., 2011). In moss, bulge formation and the direction of tip growth are determined by a dynamic actin-rich vesicle cluster that directs secretion to defined cortical locations at the apex where the cell wall will selectively yields (Bibeau et al., 2017; Furt et al., 2013; Vidali et al., 2009; Wu and Bezanilla, 2018). The actin-filament nucleators and actin-binding proteins that assemble the actin-rich cluster are being identified (Bascom et al., 2018).

The importance of microtubules for sustained tip growth in moss was established long ago (Doonan et al., 1988). At least, two kinesin motor proteins are required to generate a microtubule array that coalesces at the actin-rich vesicle cluster and maintain a stable tip-growing cell (Hiwatashi et al., 2014; Yamada and Goshima, 2018). Interestingly, a MYOSINVIII mutant displays ectopic branch initiation/bulge formation with some cells having multiple bulges (Wu et al., 2011). Interestingly, MYOSINVIII is an actin-based motor that loca-

lizes to microtubule plus ends, and appears to form functional linkages between the microtubule and actin cytoskeletal systems (Wu and Bezanilla, 2018).

6. A finite element model of root hair initiation

To understand how mechanical cues on the cell wall affect microtubules and bulge formation, Krupinski et al. created an FE model to simulate local cell wall loosening and outgrowth (Krupinski et al., 2016). The cell wall was simulated as a standard isotropic elastic material with thin shell geometry subject to continuous turgor pressure. Biomechanical and mechanical parameters were analyzed. For a biochemical factor, ROP activation was simulated as a function of an auxin gradient. Consistent with experimental observation, the active ROP pattern converged to a patch and localized to the basal end of the outer plasma membrane only in the presence of the auxin gradient (Jones et al., 2002b; Molendijk et al., 2001), indicating that auxin-dependent ROP activation is a plausible mechanism to define a stable site for local outgrowth. Mechanically, they simulated the static stress pattern around the root hair initiation site. First, it was shown that a cell subject to constant turgor pressure exhibited maximal principal stress in the wall that correlated with orientations of microtubules similar to those observed in *Arabidopsis* root (Pietra et al., 2013). This implies that cell-level stress can serve as an additional stress component affecting the orientation and alignment of microtubules. They also demonstrated reduction in stress near the apical and basal ends of the epidermal cell wall with local stress manipulation, which may serve as a spatial cue to pattern root hair initiation. As shown in Fig. 5a, a square patch with a small circular region of variable stiffness was employed to represent the epidermal cell wall with a root hair initiation site. The circular region was locally loosened to mimic a process in which expansins might loosen linkages between cellulose microfibrils. This perturbation resulted in a circumferential arrangement of maximal principal stress tensors surrounding of the circular region (Fig. 5a). By contrast, stiffening the circular region, which is proposed to represent a precursor of root hair initiation leads to a distinct stress pattern with a radial distribution (Fig. 5a). This radial star-like pattern resembles microtubule orientations that were observed in vivo at the root hair

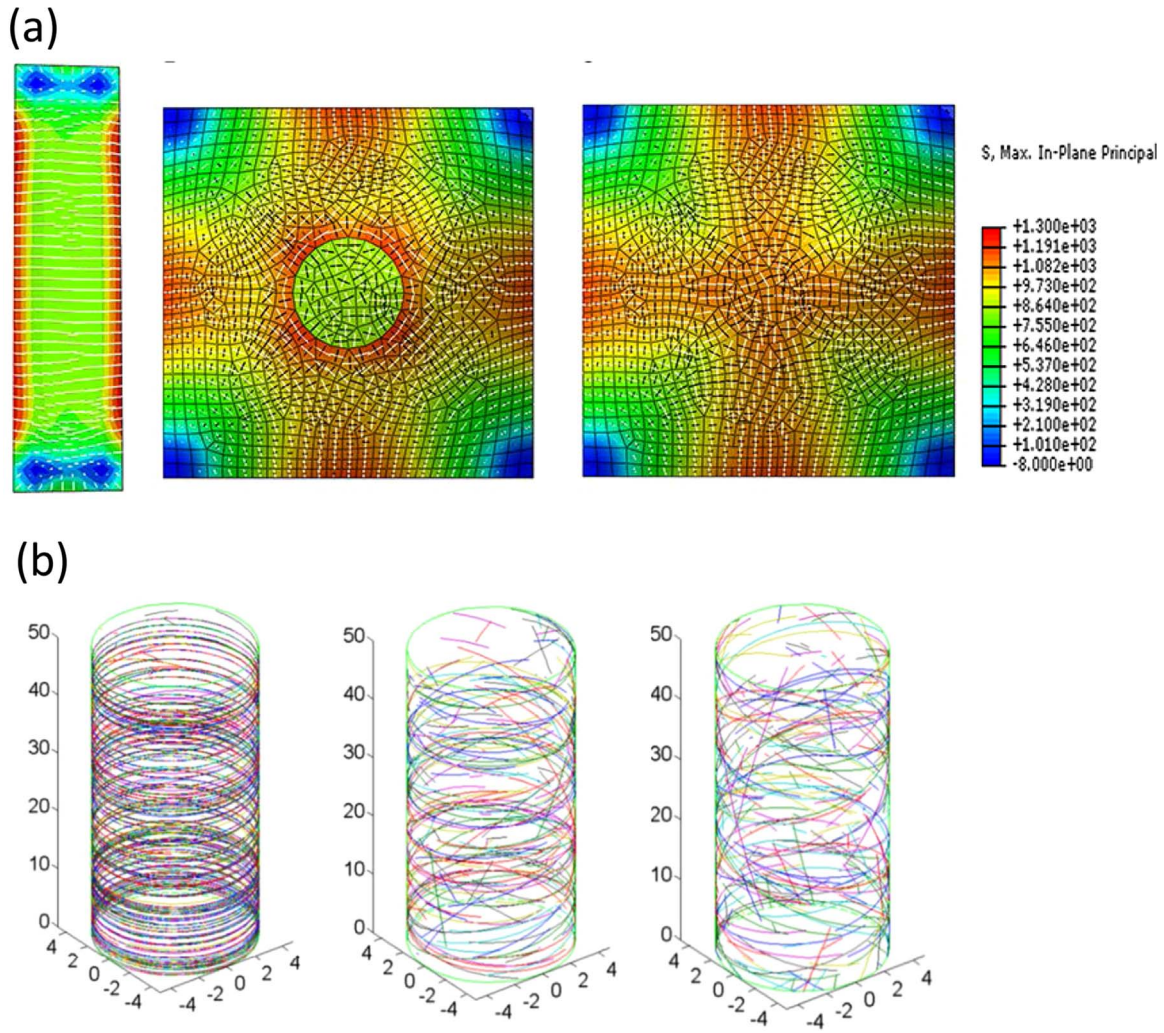

Fig. 5. Multi-scale modeling of microtubule dynamics and coupling between microtubule dynamics and external cues. (a) A multi-aspect static finite element model simulating root hair initiation process [reprinted with permission from (Krupinski et al., 2016)]. The stress pattern in a rectangular domain corresponds well to the transversely aligned cellulose fibers and microtubules in experiments. Reduction in stress at specific regions near the basal end of the cell indicates the initiation site of root hair outgrowth. A square domain of cell wall with a circular patch represents the initiation site controlled by active ROP signaling pathways. Softening the circular patch results in circumferential alignment of maximal principal stress (middle) as shown in experiments. Stiffening of the central patch leads to radial stress that might precedes the outgrowth of root hair (right). (b) A three-dimensional model incorporating microtubule dynamics with alternating boundary dynamics [reprinted with permission from (Eren et al., 2010) Copyright © 2010 by The American Society for Cell Biology]. Left: perfect alignment of cortical microtubules under a parameter set with bundling of microtubules below a critical entrainment angle. Middle: Inducing catastrophe at the boundaries still leads to formation of transverse microtubule array, but without bundling, alignment is reduced. Right: Making the boundary reflective leads to further reduction in the alignment of microtubules. This indicates that cell geometry and its effect on the catastrophe frequency near the surface have a strong influence on generation of transversely aligned microtubule array. Units in x, y, z directions are μm.

outgrowth site (Pietra et al., 2013). However, the prediction for local cell wall stiffening has not been validated, and the detailed behaviors of the microtubule cytoskeleton have not been statistically analyzed. For example, it will be important to quantify the extent to which the microtubule array is radial prior to bulge formation, and whether or not it reliably converts to a transverse circumferential array after bulge formation.

7. Computational models of microtubule arrays: self-organization

As mentioned above, the coupling between microtubule array remodeling and cellulose microfibrils deposition is a key determinant for anisotropic expansion. However, the spatiotemporal dynamics of microtubule array are rather complex. In this regard, computational models provide an efficient means to reconstitute microtubule behaviors *in silico*, and predict which parameters (and microtubule associated proteins) are likely to be the most important in terms of organizing a cortical array at the spatial scale of the cell. These models can be adapted to the various 2D and 3D geometries that simulate cell shape and boundary effects on the cortical array.

Computational models of the plant cortical array are parameterized with accurate live cell imaging data. In the plant cortex, the dynamics of individual microtubules can be easily tracked, including key parameters such as of treadmilling rate which accounts for growth and depolymerization and catastrophe/rescue frequencies (Ehrhardt and Shaw, 2006; Shaw et al., 2003a). The organization of the cortical array is also influenced by deterministic events that depend on physical interactions between microtubules. Angle-dependent interactions between microtubules are powerful determinants of array organization (Hawkins et al., 2010) or catastrophe (Chi and Ambrose, 2016; Tindemans et al., 2010). When a polymerizing plus end of one microtubule makes contact to the other microtubule, different events can take place depending on an angle between the orientations of two microtubules. If the angle is smaller than a threshold, the plus end of the growing microtubule changes a direction to polymerize in a direction parallel to the other microtubule, called zippering and bundling (Dixit and Cyr, 2004). If the angle is greater than the threshold, the collision can induce catastrophe by causing the plus end to switch from a mode of polymerization to depolymerization (Chi and Ambrose, 2016; Tindemans et al., 2010). Alternatively, microtubules can also cross over one another. This crossover arrangement of microtubules presents a preferred substrate for katanin-dependent severing (Lindeboom et al., 2013; Wightman and Turner, 2007; Zhang et al., 2013c).

The earliest microtubule model introduced significance of the zippering and bundling of microtubules induced by collisions (Dixit and Cyr, 2004). The bundling of microtubules is believed to be facilitated and strengthened by the microtubule-associated proteins that provide stability by crosslinking ability (Stoppin-Mellet et al., 2013). Baulin et al. used a minimal model to show that perturbing the plus-end polymerization of microtubules leads to constrained growth where an increase in a polymerization rate would also affect frequency of collision between neighboring microtubules, and orientation cues can mediate network reorientation and ordered alignment (Baulin et al., 2007). However, it failed to consider known key parameters such as collision-induced catastrophe and crossover events. At molecular level, these aforementioned dynamics are highly dependent on collision angles between microtubules, which have been investigated and confirmed by a two-dimensional (2D) mechanochemical model, which accounts for the chemical bonding of microtubule anchoring and crosslinking proteins in addition to the mechanistic description of microtubule entrainment (Allard et al., 2010a). It is noteworthy that both ends of microtubules showed persistent phases of growth, pause, and depolymerization (Shaw et al., 2003a). However, earlier models usually overlooked the transition between the three phases for simplicity, by including growth and depolymerization only (two-state). A more realistic 2D model incorporated three-state dynamic instability of microtubules - polymerization, depolymerization, and a pausing state - at the plus end of microtubules (Allard et al., 2010b). They found that the plus-end zippering significantly enhanced the ordering of microtubules, and simulated boundary-induced catastrophe is able to fine-tune the dominant orientation of microtubules to be transverse to the orientation of a cell's growth axis. Specifically, when microtubules collide with the top and bottom of the 2D square domain, catastrophe is triggered, and this results in dominant transverse angles in all simulations. Mace et al. extended the model (Allard et al., 2010b) by simulating katanin-induced severing of microtubules at crossover points and showed that this dynamic model coupled with low level of collision-induced catastrophe is sufficient to enhance the ordering of the microtubule array (Mace and Wang, 2015). A more recent model recapitulated the role of katanin-mediated severing and confirmed that selective severing only at crossover points, instead of random and uniform severing, could promote the ordering of microtubules (Deinum et al., 2017). However, to enhance the ordering of microtubules, severing at crossover points still requires zippering to prevent frequent severing at small encounter angles. The alignment of microtubules can also be sensitive to the geometry of tubulin-based nucleation dynamics. There are three types of nucleation events that occur on a mother microtubule. Sideways branching refers to the event when a microtubule nucleates and branches off from a mother microtubule at a specific angle of ~45° (Murata et al., 2005). Forward nucleation occurs when a new microtubule nucleates on a mother microtubule and grows toward the plus end of a mother microtubule while backward nucleation points toward the minus end. Experiments, in which plus-end marker protein EB1 was used to label microtubules, have shown predominant branching nucleation events while forward and backward nucleations are still significant (Chan et al., 2009). However, data presented by another experiment at the periclinal cell surface suggest that changes of nucleation modes of microtubules might not be involved the reorganization of microtubule array (Atkinson et al., 2014).

Deinum et al. also investigated effects of three types of microtubule-bound nucleation and concluded that the ordering of microtubule array can be enhanced mainly by directing co-alignment of newly nucleated microtubules with existing microtubules while sideways branching nucleation strengthens the effect (Deinum et al., 2011). It is possibly due to the fact that the branching nucleation of a new microtubule is often directionally biased towards the plus end of mother microtubules (Chan et al., 2009). In this regard, polarity-biased growth of microtubules provides potential influences on remodeling and emergence of ordered microtubule array.

8. Computational models of microtubule arrays with consideration of cell geometry

To overcome the limitation of microtubule dynamics in a two-dimensional constrained geometry and to link the microtubule array to a more realistic cell geometry, Eren et al. developed a three-dimensional simulation to further test the role of angle-dependent zippering and boundary-induced catastrophe for increased ordering of microtubules (Eren et al., 2010). In a case with zippering below an optimal angle threshold, perfect alignment was observed with a highly ordered microtubule array, where a dominant transverse orientation evolved (Fig. 5b). By contrast, the absence of the angle-dependent zippering dynamics reduced the ordering of microtubule array, regardless of the boundary conditions (Fig. 5b). Additionally, the boundary-induced

catastrophe was also an important factor that leads to transversely aligned microtubule array. Overall, these computational studies with coarse-grained descriptions of microtubules contribute to a systematic understanding of how intracellular microtubule dynamics and their interactions induce specific ordering of microtubule array.

Typically, plant cells have well-defined faces which are relatively flat. Their cell edges are usually characterized by high curvature; however recently divided cells generate orthogonal cross walls with a small radius of curvature relative to the previously existing cell edges (Korn, 1980). In expanding root cells, the probability of catastrophe increases at cell edges with the smallest radius of curvature between the two cell faces (Ambrose et al., 2011). Also, the effect of the curved edge and its sharpness on the kinetics of microtubules can be seen as a bias or barrier constraining microtubule polymerization independent of catastrophe. In the model developed by Baulin et al., a simplified version of collision-induced blocking between microtubules and directional bias was able to orient microtubules (Baulin et al., 2007), reminiscent of a geometrical barrier for microtubule growth. The geometrical bias or barrier is ubiquitous and inevitable as microtubules polymerize into close proximity to the cell boundaries (Cortes et al., 2006), and it would affect inter-microtubule interactions for self-organization. Therefore, it has been proposed that regions with high curvature at the interfacial boundaries of cell edges could affect microtubule dynamics. Microtubules are stiff with a persistence length of several millimeters (Feizabadi and Winton, 2013; Howard and Hyman, 2003). Due to their low flexibility, it is possible that their stability is sensitive to smoothness of local cell curvature. To test for interactions between microtubules with geometrical cues, a study combining live cell imaging and computational models predicted strong effects of a cell-edge-localized microtubule-associated protein CLASP on microtubule organization (Ambrose et al., 2011). The results indicate that microtubule depolymerization was more likely to occur when the microtubule encountered sharp edges of cells. In roots, CLASP accumulated at sharp edges and promoted localized microtubule stabilization (Ambrose et al., 2011). The proposed function of CLASP is to conditionally buffer the microtubule system against the geometric effects of cell edge sharpness and cell shape to allow transfacial microtubule bundles to form along all cell faces. This activity may be linked to the regulated synthesis of cellulose fibers that span the anticlinal and periclinal faces of the cell wall. In expanding lobed epidermal pavement cells CLASP accumulation was correlated with the radius of curvature between edges (Ambrose et al., 2011). However, the protein accumulated unevenly along a large fraction of the cell perimeter in young pavement cells, and it is not clear if cell edge sharpness is a sufficient geometric cue to recruit CLASP. CLASP mutants display a hyper-aligned microtubule array for two reasons. Sharp edge induced catastrophe orients the microtubule array parallel to the edge (Ambrose et al., 2011), and reduced cortical attachment of microtubules in the mutant allows a polymerizing microtubule to adopt variable angles of approach to an existing microtubule leading to increased parallel bundling (Ambrose and Wasteneys, 2008). The connections between *clasp* microtubule defects and the altered branching morphogenesis of trichomes and pavement cells remain unclear (Kirik et al., 2007).

Another study developed a three-dimensional computational framework to study effects of geometrical constraint on the alignment of microtubules (Chakrabortty et al., 2018). With the advantage of transforming real cell confocal images into a three-dimensional triangulated mesh, the model has the capability of adopting the geometry of a relatively wide range of plant cells. The study reproduced some of the observed distributions of microtubules using Arabidopsis leaf pavement cell geometry, consistent with their experimental observations. However, the model is incapable of explaining the extreme variability of microtubule patterns that are observed in a single leaf pavement over time (Armour et al., 2015; Belteton et al., 2018; Zhang et al., 2011). A similar recent study focused on the dependence of microtubule localization and alignment on variations in cell geometry and surface properties, in a symmetric ellipsoidal domain (Mirabet et al., 2018). In addition, external mechanical cues implemented as a direction bias also induced changes in the global orientation of microtubules. Microtubule anchoring to the plasma membrane was simulated by biasing polymerization of microtubules located closely to the boundary in a direction aligned with the boundary curvature. The directional cue of polymerization could represent changes caused by cell polarization or external tension, but it remains artificial. Smooth curvature and strong membrane-microtubule anchoring enhanced the ordering of the microtubule array but increased the anisotropy. Bundle structure and the network anisotropy are minimally affected by a change in the global cell geometry from a cubical domain to square or long rectangular one with high aspect ratio.

In all, computational models at multiple levels consider two major factors for governing microtubule dynamics. While microtubules align with principal stress, they are also sensitive to geometrical effects in terms of their self-organization. A model with higher complexity combining the aforementioned mechanical feedback and geometrical effects would be ideal for investigating the mechanism underlying the microtubule-based cell wall remodeling.

9. Cell wall stress and microtubule alignment

The biophysical properties of the cell wall have long been hypothesized to influence the organization of the microtubule cytoskeleton (Green, 1962; Landrein and Hamant, 2013), and these activities are likely important during cell branching. The magnitude and direction of in plane cell wall stress tensors are related to the geometry of the cell (radius, local curvature, cell wall thickness (Jordan and Dumais, 2010)), and the existence of neighboring adherent cells with opposing cell walls minimize tension forces in the wall (Kutschera and Briggs, 1988). This is an important concept because it provides a plausible mechanism for feedback control from the cell wall to the microtubule cytoskeleton, and provides a mechanism for cells or groups of cells to "sense" their shape or strain behaviors and modify the microtubule-cellulose microfibril networks accordingly. During branch morphogenesis in leaf hairs, cell wall stress-mediated feedback control from the cell wall to the microtubule cytoskeleton has been proposed to coordinate cell shape with the geometry of an apical microtubule depletion zone (Yanagisawa et al., 2018, 2015). There are several reports in which the subcellular distributions of microtubules correlate with the predicted patterns of cell wall stress tensors (Hamant et al., 2008; Jacques et al., 2013; Sampathkumar et al., 2014).

In general, the mechanisms by which cell wall stress is coupled to microtubule organization is poorly understood. It has been suggested that a bias in the microtubule orientations caused by a change in stress intensity is a direct consequence of the modification in the KATANIN-mediated severing activity of microtubules (Uyttewaal et al., 2012). The observation that microtubule array reorientation in response to stress tensors is delayed in a *katanin* mutant is consistent with this hypothesis; however, the mechanical linkages between the wall and KATANIN activity are not known. The mechanical feedback between cell geometry, the resultant cell wall stress pattern, and the subcellular organization of the microtubules cytoskeleton has also been simulated in *Arabidopsis* highly lobed pavement cells using a static non-linear FE model (Sampathkumar et al., 2014). Static images showed that microtubule orientations correlated with simulated cell wall stress pattern when cells were ablated or in cells that surrounded subsets of stomates. In lobed cells, subsets of microtubules were aligned with stress patterns. Several papers have pointed to a correlation between

the presence of an organized microtubule array at the convex indented regions of lobed cells (Panteris and Galatis, 2005). However, in Arabidopsis leaf pavement cells, it is clear that not all convex regions of individual cells have an organized microtubule array (Qiu et al., 2002; Zhang et al., 2011), and time-lapsed analyses indicate that the microtubule network is highly unstable, even in lobed cells that are expanding quite symmetrically (Belteton et al., 2018; Zhang et al., 2011). In this area of research, it will be important to more thoroughly validate the simulated stress patterns of cells with complex shapes that exist in the context of a tissue. It would also be important to more rigorously analyze how microtubules respond to cell wall stress patterns.

9. Conclusions and future challenges

Cell branching is widespread in the plant kingdom, and allows cells to carry out specialized mechanical functions. The cytoskeleton-dependent patterning of local cell wall heterogeneities drives polarized growth, and genetic approaches in many plant species are identifying dozens of genes that specify cortical sites for polarized growth and sculpt the slowly emerging cell form. Quantitative long-term time lapse imaging provides a graphing system at multiple spatial scales to analyze the order and interdependencies of protein function in cells with any shape (Belteton et al., 2018; Furt et al., 2013; McKenna et al., 2009; Wu et al., 2016; Yanagisawa et al., 2015). There are growing opportunities to combine multi-scale imaging approaches with FE computational modeling of the cell wall. This is an effective strategy because the molecular structure and rheology of the plant cell wall are poorly understood, and FE modeling presents an effective top-down modeling approach to predict the location and type of cell wall heterogeneities that underlie polarized growth. The complexity of the FE model and the extent to which it accurately mimics a true plant cell wall varies greatly among experiments (Bidhendi and Geitmann, 2018), and depends somewhat on the goals of the particular study. However, useful FE-model based predictions require plausible models, and there is much room for improvement. Static FE models predict patterns of cell wall stress (Fig. 4c) that depend strongly on the material properties of the shell (Fayant et al., 2010; Sampathkumar et al., 2014; Yanagisawa et al., 2015). However, these predictions should be interpreted with caution because direct methods to validate the patterns of in-plane cell wall stress do not exist. FE models that simulate growth include a shell re-meshing and cell wall parameter resetting steps between cycles that ignore important cytoplasmic controls. For example, cell wall thickness resetting can generate wall delivery maps (Fig. 4c), but the spatial patterns of secretion, localized cell-wall modification, and known nanoscale variability in cell wall thickness are ignored. Each of these weaknesses could be addressed with improved models. The inclusion of a fiber-reinforced matrix was an important advance to quantify clear thresholds for cellulose-fiber based alignment during highly anisotropic diffuse growth (Yanagisawa et al., 2015). However, in the model, fiber angle distributions are assigned during re-meshing as a function of cell geometry. This ignores the fact that the cortical microtubule array, the dynamics of which operate at the time scale of seconds, patterns cellulose microfibril angle distributions. Along similar lines, it is often hypothesized that subcellular patterns of cell wall stress feed back on the microtubule cytoskeleton to influence cell morphogenesis (Sampathkumar et al., 2014). However, microtubule networks are highly unstable, and highly variable in pavement cells at all developmental stages. Statistical analyses of predicted cell wall stress patterns and microtubule alignment over time would help to clarify which microtubules respond to stress and have power to alter cell shape. Because stress-mediated feedback control on the microtubule system is hypothesized to play such an important role in morphogenesis, there is a strong need to determine how microtubules respond to cell wall tensile stress and how wall stress is physically linked to microtubules. Integrated multi-scale models of microtubule dynamics and cell wall stress could accelerate the search for protein activities that link these two important cellular systems. Further development and combined use multivariate live cell imaging and FE modeling can be used to efficiently reveal systems-level controls and accelerate engineering strategies to specify plant phenotypes that have an agronomic importance.

Acknowledgements

This work was supported by the National Science Foundation MCB grant no. 1715544 to D.B.S.

References

Allard, J.F., Ambrose, J.C., Wasteneys, G.O., Cytrynbaum, E.N., 2010a. A mechanochemical model explains interactions between cortical microtubules in plants. Biophys. J. 99, 1082–1090.
Allard, J.F., Wasteneys, G.O., Cytrynbaum, E.N., 2010b. Mechanisms of self-organization of cortical microtubules in plants revealed by computational simulations. Mol. Biol. Cell 21, 278–286.
Ambrose, C., Allard, J.F., Cytrynbaum, E.N., Wasteneys, G.O., 2011. A CLASP-modulated cell edge barrier mechanism drives cell-wide cortical microtubule organization in Arabidopsis. Nat. Commun. 2, 430.
Ambrose, J.C., Wasteneys, G.O., 2008. CLASP modulates microtubule-cortex interaction during self-organization of acentrosomal microtubules. Mol. Biol. Cell 19, 4730–4737.
Arioli, T., Peng, L., Betzner, A.S., Burn, J., Wittke, W., Herth, W., Camilleri, C., Hofte, H., Plazinski, J., Birch, R., Cork, A., Glover, J., Redmond, J., Williamson, R.E., 1998. Molecular analysis of cellulose biosynthesis in *Arabidopsis*. Science 279, 717–720.
Armour, W.J., Barton, D.A., Law, A.M., Overall, R.L., 2015. Differential growth in periclinal and anticlinal walls during lobe formation in Arabidopsis cotyledon pavement cells. Plant Cell 27, 2484–2500.
Atkinson, S., Kirik, A., Kirik, V., 2014. Microtubule array reorientation in response to hormones does not involve changes in microtubule nucleation modes at the periclinal cell surface. J. Exp. Bot. 65 (20), 5867–5875.
Baluska, F., Salaj, J., Mathur, J., Braun, M., Jasper, F., Samaj, J., Chua, N.H., Barlow, P.W., Volkmann, D., 2000. Root hair formation: f-actin-dependent tip growth is initiated by local assembly of profilin-supported F-actin meshworks accumulated within expansin-enriched bulges. Dev. Biol. 227, 618–632.
Bascom, C.S., Jr., Hepler, P.K., Bezanilla, M., 2018. Interplay between ions, the cytoskeleton, and cell wall properties during tip growth. Plant Physiol. 176, 28–40.
Baskin, T.I., 2005. Anisotropic expansion of the plant cell wall. Annu. Rev. Cell Dev. Biol. 21, 203–222.
Basu, D., Le, J., Zakharova, T., Mallery, E.L., Szymanski, D.B., 2008. A SPIKE1 signaling complex controls actin-dependent cell morphogenesis through the heteromeric WAVE and ARP2/3 complexes. Proc. Natl. Acad. Sci. USA 105, 4044–4049.
Baulin, V.A., Marques, C.M., Thalmann, F., 2007. Collision induced spatial organization of microtubules. Biophys. Chem. 128, 231–244.
Beilstein, M., Szymanski, D., 2004. Cytoskeletal requirements during *Arabidopsis* trichome development. In: Hussey, P. (Ed.), The Plant Cytoskeleton in Cell Differentiation and Development. Blackwell, Oxford, UK, 265–289.
Belteton, S., Sawchuk, M.G., Donohoe, B.S., Scarpella, E., Szymanski, D.B., 2018. Reassessing the roles of PIN proteins and anticlinal microtubules during pavement cell morphogenesis. Plant Physiol. 176, 432–449.
Bibeau, J.P., Kingsley, J.L., Furt, F., Tuzel, E., Vidali, L., 2017. F-actin Meditated focusing of vesicles at the cell tip Is essential for polarized growth. Plant Physiol..
Bibikova, T.N., Jacob, T., Dahse, I., Gilroy, S., 1998. Localized changes in apoplastic and cytoplasmic pH are associated with root hair development in Arabidopsis thaliana. Development 125, 2925–2934.
Bidhendi, A.J., Geitmann, A., 2018. Finite element modeling of shape changes in plant cells. Plant Physiol. 176, 41–56.
Bosch, M., Cheung, A.Y., Hepler, P.K., 2005. Pectin methylesterase, a regulator of pollen tube growth. Plant Physiol. 138, 1334–1346.
Burk, D.H., Liu, B., Zhong, R., Morrison, W.H., Ye, Z.H., 2001. A Katanin-like protein regulates normal cell wall biosynthesis and cell elongation. Plant Cell 13, 807–827.
Burn, J.E., Hurley, U.A., Birch, R.J., Arioli, T., Cork, A., Williamson, R.E., 2002. The cellulose-deficient Arabidopsis mutant rsw3 is defective in a gene encoding a putative glucosidase II, an enzyme processing N-glycans during ER quality control. Plant J. 32, 949–960.
Buschmann, H., Lloyd, C.W., 2008. *Arabidopsis* mutants and the network of microtubule-associated functions. Mol. Plant 1, 888–898.
Carol, R.J., Dolan, L., 2006. The role of reactive oxygen species in cell growth: lessons from root hairs. J. Exp. Bot. 57, 1829–1834.
Carol, R.J., Takeda, S., Durrant, M.C., Kakesova, H., Derbyshire, P., Drea, S., V, Z., Dolan, L., 2005. A RhoGDP dissociation inhibitor spatially regulates growth in root hair cells. Nature 438, 1013–1016.
Chakrabortty, B., Blilou, I., Scheres, B., Mulder, B.M., 2018. A computational framework for cortical microtubule dynamics in realistically shaped plant cells. PLoS Comput. Biol. 14, e1005959.

Chan, J., Sambade, A., Calder, G., Lloyd, C., 2009. Arabidopsis cortical microtubules are initiated along, as well as branching from, existing microtubules. Plant Cell 21, 2298–2306.
Chi, Z., Ambrose, C., 2016. Microtubule encounter-based catastrophe in Arabidopsis cortical microtubule arrays. BMC Plant Biol. 16, 18.
Cho, H.T., Cosgrove, D.J., 2002. Regulation of root hair initiation and expansin gene expression in Arabidopsis. Plant Cell 14, 3237–3253.
Cortes, S., Glade, N., Chartier, I., Tabony, J., 2006. Microtubule self-organisation by reaction-diffusion processes in miniature cell-sized containers and phospholipid vesicles. Biophys. Chem. 120, 168–177.
Cosgrove, D.J., 1993. Water uptake by growing cells: an assessment of the controlling roles of wall relaxation, solute uptake and hydraulic conductance. Int. J. Plant Sci. 154, 10–21.
Cosgrove, D.J., 2000. Loosening of plant cell walls by expansins. Nature 407, 321–326.
Cosgrove, D.J., 2005. Growth of the plant cell wall. Nat. Rev. Mol. Cell Biol. 6, 850–861.
Cosgrove, D.J., 2018. Diffuse growth of plant cell walls. Plant Physiol. 176, 16–27.
Cove, D.J., Knight, C.D., 1993. The Moss Physcomitrella patens, a model system with potential for the study of plant reproduction. Plant Cell 5, 1483–1488.
Deinum, E.E., Tindemans, S.H., Lindeboom, J.J., Mulder, B.M., 2017. How selective severing by katanin promotes order in the plant cortical microtubule array. Proc. Natl. Acad. Sci. USA 114, 6942–6947.
Deinum, E.E., Tindemans, S.H., Mulder, B.M., 2011. Taking directions: the role of microtubule-bound nucleation in the self-organization of the plant cortical array. Phys. Biol. 8, 056002.
Dixit, R., Cyr, R., 2004. Encounters between dynamic cortical microtubules promote ordering of the cortical array through angle-dependent modifications of microtubule behavior. Plant Cell 16, 3274–3284.
Dobney, S., Chiasson, D., Lam, P., Smith, S.P., Snedden, W.A., 2009. The calmodulin-related calcium sensor CML42 plays a role in trichome branching. J. Biol. Chem. 284, 31647–31657.
Dolan, L., Janmaat, K., Willemsen, V., Linstead, P., Poethig, S., Roberts, K., Scheres, B., 1993. Cellular organisation of the *Arabidopsis thaliana* root. Development 119, 71–84.
Doonan, J.H., Cove, D.J., Lloyd, C.W., 1988. microtubules and microfilaments in tip growth - evidence that microtubules impose polarity on protonemal growth in Physcomitrella-patens. J. Cell Sci. 89, 533–540.
Ehrhardt, D.W., Shaw, S.L., 2006. Microtubule dynamics and organization in the plant cortical array. Annu. Rev. Plant Biol. 57, 859–875.
Eren, E.C., Dixit, R., Gautam, N., 2010. A three-dimensional computer simulation model reveals the mechanisms for self-organization of plant cortical microtubules into oblique arrays. Mol. Biol. Cell 21, 2674–2684.
Esau, K., 1977. Anatomy of Seed Plants 2d ed.. Wiley, New York.
Exner, V., Gruissem, W., Hennig, L., 2008. Control of trichome branching by chromatin assembly factor-1. BMC Plant Biol. 8, 54.
Falbel, T.G., Koch, L.M., Nadeau, J.A., Segui-Simarro, J.M., Sack, F.D., Bednarek, S.Y., 2003. SCD1 is required for cell cytokinesis and polarized cell expansion in *Arabidopsis thaliana*. Development 130, 4011–4024.
Fayant, P., Girlanda, O., Chebli, Y., Aubin, C.E., Villemure, I., Geitmann, A., 2010. Finite element model of polar growth in pollen tubes. Plant Cell 22, 2579–2593.
Feizabadi, S.M.B., J., Winton, C., 2013. Analysis of a single soybean microtubule's persistence length. Adv. Biosci. Biotechnol. 4, 930–936.
Feng, Y., Xu, P., Li, B.S., Li, P.P., Wen, X., An, F.Y., Gong, Y., Xin, Y., Zhu, Z.Q., Wang, Y.C., Guo, H.W., 2017. Ethylene promotes root hair growth through coordinated EIN3/EIL1 and RHD6/RSL1 activity in Arabidopsis. Proc. Natl. Acad. Sci. USA 114, 13834–13839.
Foard, D.E., Haber, A.H., 1961. Anatomic studies of gamma-irradiated wheat growing without cell division. Am. J. Bot. 48, 438–446.
Folkers, U., Kirik, V., Schöbinger, U., Falk, S., Krishnakumar, S., Pollock, M.A., Oppenheimer, D.G., Day, I., Reddy, A.R., Jürgens, G., Hülskamp, M., 2002. The cell morphogenesis gene *ANGUSTIFOLIA* encodes a CtBP/BARS-like protein and is involved in the control of the microtubule cytoskeleton. EMBO 21, 1280–1288.
Foreman, J., Demidchik, V., Bothwell, J.H.F., Mylona, P., Miedma, H., Torres, M.A., Linstead, P., Costa, S., Brownlee, C., Jones, J.D.G., Davies, J.M., Dolan, L., 2003. Reactive oxygen species produced by NADPH oxidase regulate plant cell growth. Nature 422, 442–446.
Forouzesh, E., Goel, A., Mackenzie, S.A., Turner, J.A., 2013. In vivo extraction of Arabidopsis cell turgor pressure using nanoindentation in conjunction with finite element modeling. Plant J. 73, 509–520.
Fujita, M., Himmelspach, R., Ward, J., Whittington, A., Hasenbein, N., Liu, C., Truong, T.T., Galway, M.E., Mansfield, S.D., Hocart, C.H., Wasteneys, G.O., 2013. The *anisotropy1* D604N mutation in the Arabidopsis cellulose synthase1 catalytic domain reduces cell wall crystallinity and the velocity of cellulose synthase complexes. Plant Physiol. 162, 74–85.
Furt, F., Liu, Y.C., Bibeau, J.P., Tuzel, E., Vidali, L., 2013. Apical myosin XI anticipates F-actin during polarized growth of Physcomitrella patens cells. Plant J. 73, 417–428.
Green, P.B., 1962. Mechanisms for plant cellular morphogenesis. Science 138, 1404–1405.
Grierson, C., Nielsen, E., Ketelaarc, T., Schiefelbein, J., 2014. Root hairs 12. The Arabidopsis Book/American Society of Plant Biologists, e0172.
Grierson, C.S., Roberts, K., Feldmann, K.A., Dolan, L., 1997. The COW1 locus of arabidopsis acts after RHD2, and in parallel with RHD3 and TIP1, to determine the shape, rate of elongation, and number of root hairs produced from each site of hair formation. Plant Physiol. 115, 981–990.
Gutierrez, R., Lindeboom, J.J., Paredez, A.R., Emons, A.M., Ehrhardt, D.W., 2009. Arabidopsis cortical microtubules position cellulose synthase delivery to the plasma membrane and interact with cellulose synthase trafficking compartments. Nat. Cell Biol. 11, 797–806.
Hamant, O., Heisler, M.G., Jonsson, H., Krupinski, P., Uyttewaal, M., Bokov, P., Corson, F., Sahlin, P., Boudaoud, A., Meyerowitz, E.M., Traas, J., 2008. Developmental patterning by mechanical signals in *Arabidopsis*. Science 322, 1650–1655.
Hawkins, R.J., Tindemans, S.H., Mulder, B.M., 2010. Model for the orientational ordering of the plant microtubule cortical array. Phys. Rev. E Stat. Nonlinear Soft Matter Phys. 82, 011911.
Hayot, C.M., Forouzesh, E., Goel, A., Avramova, Z., Turner, J.A., 2012. Viscoelastic properties of cell walls of single living plant cells determined by dynamic nanoindentation. J. Expt. Bot. 63, 2525–2540.
Hepler, P.K., Newcomb, E.H., 1964. Microtubules and fibrils in the cytoplasm of *Coleus* cells undergoing secondary wall deposition. J. Cell Biol. 20, 529–532.
Hepler, P.K., Rounds, C.M., Winship, L.J., 2013. Control of cell wall extensibility during pollen tube growth. Mol. Plant 6, 998–1017.
Hiwatashi, Y., Sato, Y., Doonan, J.H., 2014. Kinesins have a dual function in organizing microtubules during both tip growth and cytokinesis in Physcomitrella patens. Plant Cell 26, 1256–1266.
Hocq, L., Pelloux, J., Lefebvre, V., 2017. Connecting homogalacturonan-type pectin remodeling to acid growth. Trends Plant Sci. 22, 20–29.
Honkanen, S., Dolan, L., 2016. Growth regulation in tip-growing cells that develop on the epidermis. Curr. Opin. Plant Biol. 34, 77–83.
Howard, J., Hyman, A.A., 2003. Dynamics and mechanics of the microtubule plus end. Nature 422, 753–758.
Howles, P.A., Birch, R.J., Collings, D.A., Gebbie, L.K., Hurley, U.A., Hocart, C.H., Arioli, T., Williamson, R.E., 2006. A mutation in an Arabidopsis ribose 5-phosphate isomerase reduces cellulose synthesis and is rescued by exogenous uridine. Plant J. 48, 606–618.
Hulskamp, M., Misra, S., Jürgens, G., 1994. Genetic dissection of trichome cell development in *Arabidopsis*. Cell 76, 555–566.
Ilgenfritz, H., Bouyer, D., Schnittger, A., Mathur, J., Kirik, V., Schwab, B., Chua, N.-H., Jurgens, G., Hulskamp, M., 2003. The Arabdopsis *STICHEL* gene is a regulator of trichome branch number and encodes a novel protein. Plant Physiol. 131, 643–645.
Jacques, E., Verbelen, J.P., Vissenberg, K., 2013. Mechanical stress in Arabidopsis leaves orients microtubules in a 'continuous' supracellular pattern. BMC Plant Biol. 13, 163.
Jones, M.A., Shen, J., Fu, Y., Li, H., Yang, Z., Grierson, C.S., 2002a. The Arabidopsis Rop2 GTPase is a positive regulator of both root hair initiation and tip growth. Plant Cell 14, 763–776.
Jordan, B.M., Dumais, J., 2010. Biomechanics of Plant Cell Growth, Encyclopedia of Life Sciences. John Wiley & Sons, Ltd., Chinchester.
Kasili, R., Huang, C.C., Walker, J.D., Simmons, L.A., Zhou, J., Faulk, C., Hulskamp, M., Larkin, J.C., 2011. Branchless trichomes links cell shape and cell cycle control in Arabidopsis trichomes. Development 138, 2379–2388.
Kiefer, C.S., Claes, A.R., Nzayisenga, J.C., Pietra, S., Stanislas, T., Huser, A., Ikeda, Y., Grebe, M., 2015. Arabidopsis AIP1-2 restricted by WER-mediated patterning modulates planar polarity. Development 142, 151–161.
Kijima, S.T., Staiger, C.J., Katoh, K., Nagasaki, A., Ito, K., Uyeda, T.Q.P., 2018. Arabidopsis vegetative actin isoforms, AtACT2 and AtACT7, generate distinct filament arrays in living plant cells. Sci. Rep. 8, 4381.
Kirik, V., Herrmann, U., Parupalli, C., Sedbrook, J.C., Ehrhardt, D.W., Hulskamp, M., 2007. CLASP localizes in two discrete patterns on cortical microtubules and is required for cell morphogenesis and cell division in Arabidopsis. J. Cell Sci. 120, 4416–4425.
Korn, R.W., 1980. The changing shape of plant cells: transformations during cell proliferation. Ann. Bot. 46, 649–666.
Kotchoni, S.O., Zakharova, T., Mallery, E.L., Le, J., El-Assal, S.E., Szymanski, D.B., 2009. The association of the Arabidopsis actin-related protein (ARP) 2/3 complex with cell membranes is linked to its assembly status, but not its activation. Plant Physiol. 151, 2095–2109.
Krupinski, P., Bozorg, B., Larsson, A., Pietra, S., Grebe, M., Jonsson, H., 2016. A model analysis of mechanisms for radial microtubular patterns at root hair initiation sites. Front. Plant Sci. 7, 1560.
Kusano, H., Testerink, C., Vermeer, J.E., Tsuge, T., Shimada, H., Oka, A., Munnik, T., Aoyama, T., 2008. The Arabidopsis Phosphatidylinositol Phosphate 5-Kinase PIP5K3 is a key regulator of root hair tip growth. Plant Cell 20, 367–380.
Kutschera, U., Briggs, W.R., 1988. Growth, in vivo extensibility, and tissue tension in developing pea internodes. Plant Physiol. 86, 306–311.
Landrein, B., Hamant, O., 2013. How mechanical stress controls microtubule behavior and morphogenesis in plants: history, experiments and revisited theories. Plant J. 75, 324–338.
Ledbetter, M.C., Porter, K.R., 1963. A "microtubule" in plant cell fine structure. J. Cell Biol. 19, 239–250.
Leliaert, F., Smith, D.R., Moreau, H., Herron, M.D., Verbruggen, H., Delwiche, C.F., De Clerck, O., 2012. Phylogeny and molecular evolution of the Green Algae. Crit. Rev. Plant Sci. 31, 1–46.
Leucci, M.R., Di Sansebastiano, G.-P., Gigante, M., Dalessandro, G., Piro, G., 2007. Secretion marker proteins and cell-wall polysaccharides move through different secretory pathways. Planta 225, 1001–1017.
Levesque-Tremblay, G., Pelloux, J., Braybrook, S.A., Muller, K., 2015. Tuning of pectin methylesterification: consequences for cell wall biomechanics and development. Planta 242, 791–811.
Levin, D.A., 1973. The role of trichomes in plant defense. Q Rev. Biol. 48, 3–15.
Li, S., Lei, L., Somerville, C.R., Gu, Y., 2012. Cellulose synthase interactive protein 1 (CSI1) links microtubules and cellulose synthase complexes. Proc. Natl. Acad. Sci. USA 109, 185–190.

Lin, D., Cao, L., Zhou, Z., Zhu, L., Ehrhardt, D., Yang, Z., Fu, Y., 2013. Rho GTPase signaling activates microtubule severing to promote microtubule ordering in Arabidopsis. Curr. Biol. 23, 290–297.
Lindeboom, J.J., Nakamura, M., Hibbel, A., Shundyak, K., Gutierrez, R., Ketelaar, T., Emons, A.M., Mulder, B.M., Kirik, V., Ehrhardt, D.W., 2013. A mechanism for reorientation of cortical microtubule arrays driven by microtubule severing. Science 342, 1202–1214.
Lu, L., Lee, Y.-R.J., Pan, R., Maloof, J.N., Liu, B., 2005. An internal motor kinesin is associated with the golgi apparatus and plays a role in trichome morphogenesis in *Arabidopsis*. Mol. Biol. Cell 16, 811–823.
Mace, A., Wang, W., 2015. Modelling the role of catastrophe, crossover and katanin-mediated severing in the self-organisation of plant cortical microtubules. IET Syst. Biol. 9, 277–284.
Mangano, S., Denita-Juarez, S.P., Choi, H.S., Marzol, E., Hwang, Y., Ranocha, P., Velasquez, S.M., Borassi, C., Barberini, M.L., Aptekmann, A.A., Muschietti, J.P., Nadra, A.D., Dunand, C., Cho, H.T., Estevez, J.M., 2017. Molecular link between auxin and ROS-mediated polar growth. Proc. Natl. Acad. Sci. USA 114, 5289–5294.
Marks, M.D., Wenger, J.P., Gilding, E., Jilk, R., Dixon, R.A., 2009. Transcriptome analysis of *Arabidopsis* wild-type and *gl3-sst sim* trichomes identifies four additional genes required for trichome development. Mol. Plant 2, 803–822.
Marrotte, R.R., Chmura, G.L., Stone, P.A., 2012. The utility of Nymphaeaceae sclereids in paleoenvironmental research. Rev. Palaeobot. Palynol. 169, 29–37.
Massucci, J.D., Schiefelbein, J.W., 1994. The rhd6 mutation of Arabidopsis thaliana alters root-hair initiation through an auxin- and ethylene-associated process. Plant Physiol. 106, 1335–1346.
Mathur, J., Chua, N.-H., 2000. Microtubule stabilization leads to growth reorientation in *Arabidopsis* trichomes. Plant Cell 12, 465–477.
Mathur, J., Spielhofer, P., Kost, B., Chua, N., 1999. The actin cytoskeleton is required to elaborate and maintain spatial patterning during trichome cell morphogenesis in *Arabidopsis thaliana*. Development 126, 5559–5568.
Mauricio, R., 1998. Costs of resistance to natural enemies in field populations of the annual plant *Arabidopsis thaliana*. Am. Nat. 151, 20–28.
Mazie, A.R., Baum, D.A., 2016. Clade-specific positive selection on a developmental gene: branchless TRICHOME and the evolution of stellate trichomes in Physaria (Brassicaceae). Mol. Phylogenet. Evol. 100, 31–40.
McKenna, S.T., Kunkel, J.G., Bosch, M., Rounds, C.M., Vidali, L., Winship, L.J., Hepler, P.K., 2009. Exocytosis precedes and predicts the increase in growth in oscillating pollen tubes. Plant Cell 21, 3026–3040.
Melaragno, J.E., Mehrotra, B., Coleman, A.W., 1993. Relationship between endopolyploidy and cell size in epidermal tissue of Arabidopsis. Plant Cell 5, 1661–1668.
Mirabet, V., Krupinski, P., Hamant, O., Meyerowitz, E.M., Jonsson, H., Boudaoud, A., 2018. The self-organization of plant microtubules inside the cell volume yields their cortical localization, stable alignment, and sensitivity to external cues. PLoS Comput. Biol. 14, e1006011.
Molendijk, A.J., Bischoff, F., Rajendrakumar, C.S., Friml, J., Braun, M., Gilroy, S., Palme, K., 2001. *Arabidopsis* thaliana Rop GTPases are localized to tips of root hairs and control polar growth. EMBO J. 20, 2779–2788.
Murata, T., Sonobe, S., Baskin, T.I., Hyodo, S., Hasezawa, S., Nagata, T., Horio, T., Hasebe, M., 2005. Microtubule-dependent microtubule nucleation based on recruitment of γ-tubulin in higher plants. Nat. Cell Biol. 7, 961–968.
Nestler, J., Liu, S.Z., Wen, T.J., Paschold, A., Marcon, C., Tang, H.M., Li, D.L., Li, L., Meeley, R.B., Sakai, H., Bruce, W., Schnable, P.S., Hochholdinger, F., 2014. Roothairless5, which functions in maize (Zea mays L.) root hair initiation and elongation encodes a monocot-specific NADPH oxidase. Plant J. 79, 729–740.
Oda, Y., Fukuda, H., 2012. Initiation of cell wall pattern by a Rho- and microtubule-driven symmetry breaking. Science 337, 1333–1336.
Oda, Y., Fukuda, H., 2013a. Rho of plant GTPase signaling regulates the behavior of Arabidopsis kinesin-13A to establish secondary cell wall patterns. Plant Cell 25, 4439–4450.
Oda, Y., Fukuda, H., 2013b. Spatial organization of xylem cell walls by ROP GTPases and microtubule-associated proteins. Curr. Opin. Plant Biol. 16, 743–748.
Oppenheimer, D.G., Pollock, M.A., Vacik, J., Szymanski, D.B., Ericson, B., Feldmann, K., Marks, M.D., 1997. Essential role of a kinesin-like protein in *Arabidopsis* trichome morphogenesis. Proc. Natl. Acad. Sci. USA 94, 6261–6266.
Panteris, E., Galatis, B., 2005. The morphogenesis of lobed plant cells in the mesophyll and epidermis: organization and distinct roles of cortical microtubules and actin filaments. New Phytol. 167, 721–732.
Paredez, A.R., Somerville, C.R., Ehrhardt, D.W., 2006. Visualization of cellulose synthase demonstrates functional association with microtubules. Science 312, 1491–1495.
Pietra, S., Gustavsson, A., Kiefer, C., Kalmbach, L., Horstedt, P., Ikeda, Y., Stepanova, A.N., Alonso, J.M., Grebe, M., 2013. Arabidopsis SABRE and CLASP interact to stabilize cell division plane orientation and planar polarity. Nat. Commun. 4, 2779.
Purushotham, P., Cho, S.H., Diaz-Moreno, S.M., Kumar, M., Nixon, B.T., Bulone, V., Zimmer, J., 2016. A single heterologously expressed plant cellulose synthase isoform is sufficient for cellulose microfibril formation in vitro. Proc. Natl. Acad. Sci. USA 113, 11360–11365.
Qiu, J.L., Jilk, R., Marks, M.D., Szymanski, D.B., 2002. The *Arabidopsis SPIKE1* gene is required for normal cell shape control and tissue development. Plant Cell 14, 101–118.
Ray, P.M., Green, P.B., Cleland, R.E., 1972. Role of turgor in plant cell growth. Nature 239, 163–164.
Reddy, A., Narasimhulu, S., Safadi, F., Golovkin, M., 1996. A plant kinesin heavy chain-like protein is a calmodulin-binding protein. Plant J. 10, 9–21.
Reddy, V.S., Day, I.S., Thomas, T., Reddy, A.S., 2004. KIC, a novel Ca2+ binding protein with one EF-hand motif, interacts with a microtubule motor protein and regulates trichome morphogenesis. Plant Cell 16, 185–200.
Ridge, R.W., Uozumi, Y., Plazinski, J., Hurley, U.A., Williamson, R.E., 1999. Developmental transitions and dynamics of the cortical ER of Arabidopsis cells seen with green fluorescent protein. Plant Cell Physiol. 40, 1253–1261.
Ringli, C., Baumberger, N., Diet, A., Frey, B., Keller, B., 2002. ACTIN2 is essential for bulge site selection and tip growth during root hair development of Arabidopsis. Plant Physiol. 129, 1464–1472.
Rounds, C.M., Lubeck, E., Hepler, P.K., Winship, L.J., 2011. Propidium iodide competes with Ca(2+) to label pectin in pollen tubes and Arabidopsis root hairs. Plant Physiol. 157, 175–187.
Russell, J.J., Theriot, J.A., Sood, P., Marshall, W.F., Landweber, L.F., Fritz-Laylin, L., Polka, J.K., Oliferenko, S., Gerbich, T., Gladfelter, A., Umen, J., Bezanilla, M., Lancaster, M.A., He, S., Gibson, M.C., Goldstein, B., Tanaka, E.M., Hu, C.-K., Brunet, A., 2017. Non-model model organisms. BMC Biol. 15, 55.
Sahoo, D., Baweja, P., 2015. General characteristics of algae. In: Sahoo, D., Baweja, P. (Eds.), The Algae World. Cellular Origin, Life in Extreme Habitats and Astrobiology. Springer, Dordrecht, 3–29.
Sambade, A., Findlay, K., Schaffner, A.R., Lloyd, C.W., Buschmann, H., 2014. Actin-dependent and -independent functions of cortical microtubules in the differentiation of Arabidopsis leaf trichomes. Plant Cell 26, 1629–1644.
Sampathkumar, A., Krupinski, P., Wightman, R., Milani, P., Berquand, A., Boudaoud, A., Hamant, O., Jonsson, H., Meyerowitz, E.M., 2014. Subcellular and supracellular mechanical stress prescribes cytoskeleton behavior in Arabidopsis cotyledon pavement cells. eLife 3, e01967.
Sato, Y., Kawagoe, T., Sawada, Y., Hirai, M.Y., Kudoh, H., 2014. Frequency-dependent herbivory by a leaf beetle, Phaedon brassicae, on hairy and glabrous plants of Arabidopsis halleri subsp gemmifera. Evol. Ecol. 28, 545–559.
Schnittger, A., Jürgens, G., Hülskamp, M., 1998. Tissue layer and organ specificity of trichome formation are regulated by *GLABRA1* and *TRIPTYCHON* in *Arabidopsis*. Development 125, 2283–2289.
Schreuder, M.D.J., Brewer, C.A., Heine, C., 2001. Modelled influences of non-exchanging trichomes on leaf boundary layers and gas exchange. J. Theor. Biol. 210, 23–32.
Schwab, B., Mathur, J., Saedler, R., Schwarz, H., Frey, B., Scheidegger, C., Hulskamp, M., 2003. Regulation of cell expansion by the *distorted* genes in *Arabidopsis thaliana*: actin controls the spatial organization of microtubules. Mol. Genet. Genome 269, 350–360.
Shaw, S.L., Kamyar, R., Ehrhardt, D.W., 2003a. Sustained microtubule treadmilling in Arabidopsis cortical arrays. Science 300, 1715–1718.
Singh, S.K., Fischer, U., Singh, M., Grebe, M., Marchant, A., 2008. Insight into the early steps of root hair formation revealed by the procuste1 cellulose synthase mutant of Arabidopsis thaliana. BMC Plant Biol. 8.
Stoppin-Mellet, V., Fache, V., Portran, D., Martiel, J.L., Vantard, M., 2013. MAP65 coordinate microtubule growth during bundle formation. PLoS One 8, e56808.
Suo, B.X., Seifert, S., Kirik, V., 2013. Arabidopsis GLASSY HAIR genes promote trichome papillae development. J. Exp. Bot. 64, 4981–4991.
Szymanski, D.B., 2014. The kinematics and mechanics of leaf expansion: new pieces to the Arabidopsis puzzle. Curr. Opin. Plant Biol. 22C, 141–148.
Szymanski, D.B., Cosgrove, D.J., 2009. Dynamic coordination of cytoskeletal and cell wall systems during plant cell morphogenesis. Curr. Biol. 19, R800–R811.
Szymanski, D.B., Jilk, R.A., Pollock, S.M., Marks, M.D., 1998. Control of *GL2* expression in *Arabidopsis* leaves and trichomes. Development 125, 1161–1171.
Szymanski, D.B., Lloyd, A.M., Marks, M.D., 2000. Progress in the molecular genetic analysis of trichome initiation and morphogenesis in *Arabidopsis*. Trends Plant Sci. 5, 214–219.
Szymanski, D.B., Marks, M.D., 1998. GLABROUS1 overexpression and TRIPTYCHON alter the cell cycle and trichome cell fate in Arabidopsis. Plant Cell 10, 2047–2062.
Szymanski, D.B., Marks, M.D., Wick, S.M., 1999. Organized F-actin is essential for normal trichome morphogenesis in *Arabidopsis*. Plant Cell 11, 2331–2347.
Tian, J., Han, L., Feng, Z., Wang, G., Liu, W., Ma, Y., Yu, Y., Kong, Z., 2015. Orchestration of microtubules and the actin cytoskeleton in trichome cell shape determination by a plant-unique kinesin. eLife 4.
Tindemans, S.H., Hawkins, R.J., Mulder, B.M., 2010. Survival of the aligned: ordering of the plant cortical microtubule array. Phys. Rev. Lett. 104, 058103.
Uyttewaal, M., Burian, A., Alim, K., Landrein, B., Borowska-Wykret, D., Dedieu, A., Peaucelle, A., Ludynia, M., Traas, J., Boudaoud, A., Kwiatkowska, D., Hamant, O., 2012. Mechanical stress acts via katanin to amplify differences in growth rate between adjacent cells in Arabidopsis. Cell 149, 439–451.
Vidali, L., van Gisbergen, P.A., Guerin, C., Franco, P., Li, M., Burkart, G.M., Augustine, R.C., Blanchoin, L., Bezanilla, M., 2009. Rapid formin-mediated actin-filament elongation is essential for polarized plant cell growth. Proc. Natl. Acad. Sci. USA 106, 13341–13346.
Wang, S.S., Zhu, X.N., Lin, J.X., Zheng, W.J., Zhang, B.T., Zhou, J.Q., Ni, J., Pan, Z.C., Zhu, S.H., Ding, W.N., 2018. OsNOX3, encoding a NADPH oxidase, regulates root hair initiation and elongation in rice. Biol. Plant. 62, 732–740.
Wang, T., Park, Y.B., Cosgrove, D.J., Hong, M., 2015. Cellulose-pectin spatial contacts are inherent to never-dried arabidopsis primary cell walls: evidence from solid-state nuclear magnetic resonance. Plant Physiol. 168, 871–884.
Wasteneys, G.O., Ambrose, J.C., 2009. Spatial organization of plant cortical microtubules: close encounters of the 2D kind. Trends Cell Biol. 19, 62–71.
Wightman, R., Turner, S.R., 2007. Severing at sites of microtubule crossover contributes to microtubule alignment in cortical arrays. Plant J. 52, 742–751.
Wu, S.Z., Bezanilla, M., 2018. Actin and microtubule cross talk mediates persistent polarized growth. J. Cell Biol..
Wu, S.Z., Ritchie, J.A., Pan, A.H., Quatrano, R.S., Bezanilla, M., 2011. Myosin VIII regulates protonemal patterning and developmental timing in the moss Physcomitrella patens. Mol. Plant 4, 909–921.

Wu, T.-C., Belteton, S.A., Pack, J., Szymanski, D.B., Umulis, D.M., 2016. LobeFinder: a convex-hull based method for quantitative boundary analysis of lobed plant cells. Plant Physiol. 171, 2331–2342.
Xi, A., Yang, X., Deng, M., Chen, Y., Shao, J., Zhao, J., An, L., 2018. Isolation and identification of two new alleles of STICHEL in Arabidopsis. Biochem. Biophys. Res. Commun. 499, 605–610.
Yamada, M., Goshima, G., 2018. The KCH kinesin drives nuclear transport and cytoskeletal coalescence to promote tip cell growth in Physcomitrella patens. Plant Cell 30, 1496–1510.
Yanagisawa, M., Alonso, J.M., Szymanski, D.B., 2018. Microtubule-dependent confinement of a cell signaling and actin polymerization control module regulates polarized cell growth. Curr. Biol. 28, 2459–2466.
Yanagisawa, M., Desyatova, A.S., Belteton, S., Mallery, E.M., Turner, J.A., Szymanski, D.B., 2015. Patterning mechanisms of cytoskeletal and cell wall systems during leaf trichome morphogenesis. Nat. Plant 1, 15014.
Yanagisawa, M., Zhang, C., Szymanski, D.B., 2013. ARP2/3-dependent growth in the plant kingdom: scars for life. Front. Plant Sci. 4, 1–12.
Zhang, C., Halsey, L., Szymanski, D.B., 2011. The development and geometry of shape change in Arabidopsis thaliana cotyledon pavement cells. BMC Plant Biol. 11, 27.
Zhang, C., Kotchoni, S.O., Samuels, A.L., Szymanski, D.B., 2010. SPIKE1 signals originate from and assemble specialized domains of the endoplasmic reticulum. Curr. Biol. 20, 2144–2149.
Zhang, C., Mallery, E., Reagan, S., Boyko, V.P., Kotchoni, S.O., Szymanski, D.B., 2013a. The endoplasmic reticulum is a reservoir for WAVE/SCAR regulatory complex signaling in the Arabidopsis leaf. Plant Physiol. 162, 689–706.
Zhang, C., Mallery, E., Szymanski, D.B., 2013b. ARP2/3 localization in Arabidopsis leaf pavement cells: a diversity of intracellular pools and cytoskeletal interactions. Front. Plant Biol. 4, 1–16.
Zhang, Q., Fishel, E., Bertroche, T., Dixit, R., 2013c. Microtubule severing at crossover sites by KATANIN generates ordered cortical microtubule arrays in Arabidopsis. Curr. Biol. 23, 2191–2195.
Zhou, L.H., Liu, S.B., Wang, P.F., Lu, T.J., Xu, F., Genin, G.M., Pickard, B.G., 2017. The Arabidopsis trichome is an active mechanosensory switch. Plant Cell Environ. 40, 611–621.